Stage-by-Stage Poststall Compression System Modeling Technique

M. W. Davis Jr.*
Sverdrup Technology, Inc., Arnold Air Force Base, Tennessee 37389
and
W. F. O'Brien†
Virginia Polytechnic Institute and State University, Blacksburg, Virginia 24061

A one-dimensional, stage-by-stage axial compression system mathematical model has been constructed that can describe system behavior during poststall events such as surge and rotating stall. The model uses a numerical technique to solve the nonlinear, compressible conservation equations of mass, momentum, and energy. Inputs for blade forces and shaft work are provided by a set of quasi-steady stage characteristics modified by a first-order lagging equation to simulate dynamic stage characteristics. The model was operationally verified using experimental results for a three-stage, low-speed compressor. Using the model, two studies were conducted: one to determine the effect of heat transfer due to rapid system transients on poststall system behavior, and the other to determine the effect of a possible design modification on overall system behavior. Results from these studies demonstrate the use of this modeling technique in studies of compression system poststall behavior.

Nomenclature

A = area
A_c = compressor cross-sectional area
A_q = water (unit of measure)
a = acoustic velocity
B = "B" parameter
CV = control volume
Cx, u = axial velocity
C = specific heat of conducting metal
c_p = specific heat at constant pressure
E = energy function
e = internal energy
F_B = force of compressor blading
FX = force of compressor blading and casing acting on fluid, including wall pressure area force
H = total enthalpy
IMP = impulse function
L_c = compressor length
M_T = mass flow function based on total condition
P = pressure
Q = rate of heat addition to control volume
SW = rate of shaft work
T = temperature
TR = total temperature ratio
t = time
U = wheel speed
u, Cx = axial velocity
V_p = plenum volume
W = mass flow rate
x = axial coordinate
ρ = density
τ = time constant
ϕ = flow coefficient
$\psi^P_{S\text{-}S}$ = static-to-static pressure coefficient

$$\psi^P_{S\text{-}S} = \frac{P_{se} - P_{si}}{\frac{1}{2}\rho u^2}$$

$\psi^P_{T\text{-}S}$ = total-to-static pressure coefficient

$$\psi^P_{T\text{-}S} = \frac{P_{se} - P_{Ti}}{\frac{1}{2}\rho u^2}, \text{ Forward Flow}$$

$$\psi^P_{T\text{-}S} = \frac{P_{Te} - P_{si}}{\frac{1}{2}\rho u^2}, \text{ Reversed Flow}$$

ψ^T = stage temperature coefficient (stage loading parameter)

$$\psi^T = TR - 1$$

Subscripts
B = pertaining to bleed
e = exit conditions
i = inlet conditions
ref = reference conditions
S = static condition
SS = steady-state condition
$S\text{-}S$ = static-to-static
T = total conditions
$T\text{-}S$ = total-to-static

Introduction

IN most aircraft gas turbine engines, the compression system consists of one or more aerodynamically coupled axial-flow compressors. It is the function of the compression system to increase the static pressure and density of the working fluid. Without stable aerodynamic operation, the compression system cannot deliver the desired increase in static pressure and density. During operation of axial-flow multistage compression systems in gas turbine engines and in rigs, undesired system phenomena known as surge and/or rotating stall, have been observed. Of the two types of instabilities, rotating stall is the most detrimental for aircraft gas turbine engines because of the frequently observed inability to recover to normal operation without stopping and restarting the engine. With continued engine operation, rotating stall is "nonrecoverable."

Presented as Paper 87-2088 at the AIAA/SAE/ASME/ASEE 23rd Joint Propulsion Conference, San Diego, CA, June 29–July 2, 1987; received July 16, 1988; revision received Nov. 5, 1990; accepted for publication Nov. 20, 1990.

*Project Manager, AEDC Group, MS 900.
†J. B. Jones Professor, Mechanical Engineering Dept.

Results of several related experimental investigations can be found in Refs. 1–5.

In experimental cases, results are often limited because of specific test hardware and/or economic constraints. Where more information is desired, validated compression system mathematical models can be used to provide performance and stability information not obtained during experimental testing.

Previous compression system mathematical models have been developed using lumped-volume techniques. A lumped-volume approach makes certain assumptions about compressibility within the system. More specifically, the lumped-volume model neglects Mach number effects, uses an isentropic relationship to relate the time-dependent change in density to a time-dependent change in total pressure, and uses a steady-state form of the energy equation. Initially, models (whether overall simulations or stage-by-stage) were limited in range to the onset of system instability.[6–8] Over the last decade, poststall behavior has been of more interest, which encouraged the development of numerous models capable of exhibiting aspects of surge or rotating stall.[9–12] In general, whether overall or stage-by-stage, poststall models have been developed using lumped volume techniques. The model presented in this paper removes assumptions inherent in lumped-volume models (i.e., treats compressibility explicitly) and does so on a stage-by-stage basis.

This paper describes a dynamic compression system model capable of exhibiting observed system behavior during poststall events (surge and rotating stall). In addition, the model has the capability for providing one-dimensional information on a stage-by-stage basis for detailed analysis of the surge or rotating stall event within the compressor. The stage-by-stage construction provides a means to study gas path behavior within the compression system, and also provides a means to analyze the effects of postulated hardware modifications on system behavior. Described in this paper is the compression system modeling technique and operational verification of the model. To demonstrate applicability to current system problems, the model was used in an example analysis of a typical system transient and to examine the effect of a possible hardware modification.

Methodology

A one-dimensional, time-dependent compressor modeling technique is presented to solve the non-linear form of the conservation laws. Using these forms of the conservation laws allows compressibility to be treated explicitly. The resulting model can be used for the analysis of planar, transient, and dynamic effects on compressor operation and stability.

Illustrated in Fig. 1 is a representative single-spool, multistage compressor and ducting system. Included in this system is a portion of the compressor inlet and the combustor volume. The compressor and ducting system are modeled by an overall control volume shown in Fig. 1b. The time-dependent inlet-boundary condition is the specification of total pressure and temperature. The exit-boundary condition is either the specification of static pressure or unity Mach number. The overall control volume is divided into a set of elemental control volumes.

The governing equations are derived by the application of mass, momentum, and energy conservation principles to the elemental control volume in Fig. 1c. In the compressor section, a stage elemental control volume consists of a rotor followed by a stator, and associated volume representing the complete stage. Acting on this fluid control volume is an axial-force distribution, FX, which is attributable to the effects of the compressor blading and walls of the system. In addition, the rate of heat transfer to the fluid and shaft work done on the fluid are represented by distributions, Q and SW, respectively. The mass transfer rate across boundaries other than the inlet or exit (such as in the case of interstage bleed) is represented by the distribution, W_B.

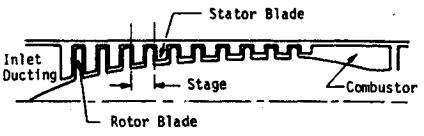

a) Compressor and ducting system

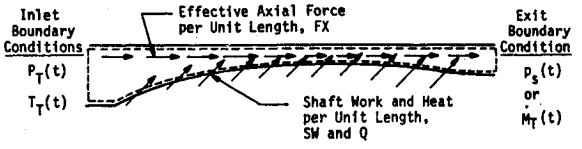

b) Overall control volume

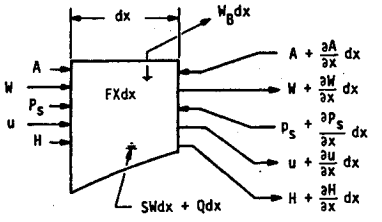

c) Elemental control volume

Fig. 1 Physical compression system modeled and control volume concepts.

Applying the continuity principle to the elemental control volume yields

$$\frac{\partial (\rho A)}{\partial t} = -\frac{\partial W}{\partial x} - W_B \tag{1}$$

where W_B is the interstage bleed flow per distributed length. Applying conservation of momentum gives

$$\frac{\partial W}{\partial t} = -\frac{\partial (IMP)}{\partial x} + FX \tag{2}$$

where

$$IMP = Wu + P_s A$$

is a momentum impulse term, and

$$FX = F_B + P_s \frac{\partial A}{\partial x}$$

is an axial-force distribution consisting of blade force and the force produced by the walls of the system.
Energy conservation yields

$$\frac{\partial (EA)}{\partial t} = -\frac{\partial H}{\partial x} - H_B + SW + Q \tag{3}$$

where

$$E = \rho(e + u^2/2); \qquad H = c_p W(T_t - T_{ref}); \qquad T_{ref} = 0$$

and H_B is the enthalpy associated with bleed flow.

To provide stage force and shaft work inputs to the momentum and energy equations, a set of quasi-steady stage characteristics must be available for input to the model. These stage characteristics provide the pressure and temperature performance for each stage as a function of the steady airflow.

A typical set of steady-state characteristics for both pre- and poststall operation is presented in Fig. 2. The stage char-

acteristics are divided into three distinct regions: prestall, rotating stall, and reversed flow. The prestall characteristic is the performance of a blade row in normal operation. The transition to a rotating stall characteristic is approximated as a continuous characteristic along a postulated throttle line. The performance in the rotating stall region is based upon a flow-weighted average of a fully developed rotating stall cell. The pressure and temperature ratios in this region represent the average pressure and temperature rise across the stage for both stalled flow and unstalled flow. The reversed-flow characteristic region represents the pressure loss and temperature rise associated with full-annulus reversed flow. The discontinuity at zero flow has been experimentally shown to exist for a three-stage low-speed compressor.[5] This aspect of the quasi-steady flow characteristic has been incorporated into the modeling technique.

The foregoing discussion of the stage characteristic has described the principal features of the prestall and reversed-flow steady-state performance, and the globally steady rotating stall average performance. For prestall and poststall reversed-flow, steady characteristics can be used as they exist. However, for a dynamic event such as rotating stall or surge, use of steady characteristics is not necessarily correct. In the rotating stall region, rotating stall develops very rapidly and the globally steady characteristic is no longer applicable. To provide a dynamic stage characteristic, a first-order time lag on the stage forces has been incorporated into the modeling technique in the rotating stall region only. The first order lag equation used is

$$\tau \frac{dFX}{dt} + FX = FX_{ss} \tag{4}$$

where

FX = blade force and pressure area force of the casing

FX_{ss} = steady-state force

τ = time constant

This lagging technique has been previously applied to several models using overall compression system characteristics.[10-12]

The governing equations of the compressor modeling technique are solved numerically using the second-order accurate MacCormack explicit finite difference scheme.[13]

The compressor model is not only an initial value problem but a boundary problem as well. Because the treatment of the boundaries can be a cause of stability problems, method-of-characteristics (MOC) boundary formulations were employed. The numerical computational volume is divided into three areas: inlet, exit, and interior. MacCormack's scheme is applied in the interior; the MOC scheme is applied at the inlet; and either an MOC scheme for unchoked flow or an

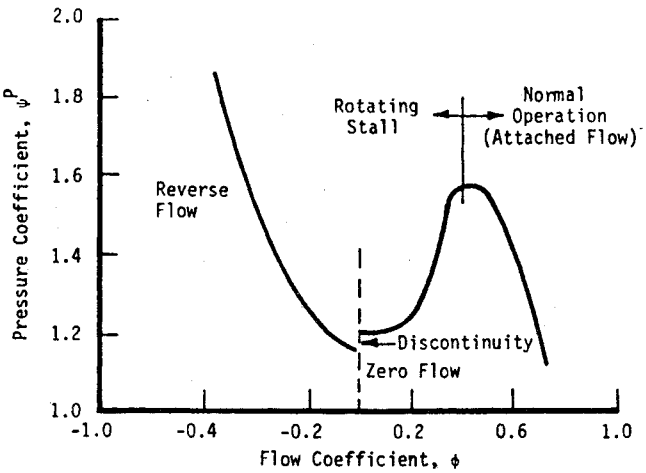

a) Pressure coefficient

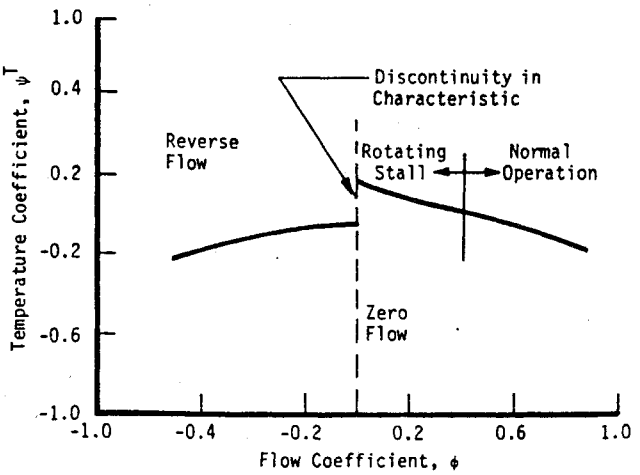

b) Temperature coefficient

Fig. 2 Typical stage characteristics.

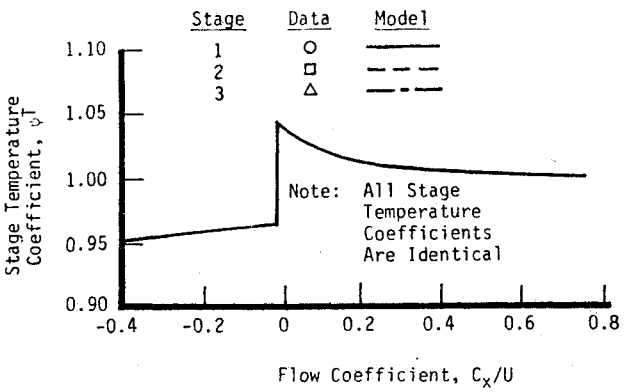

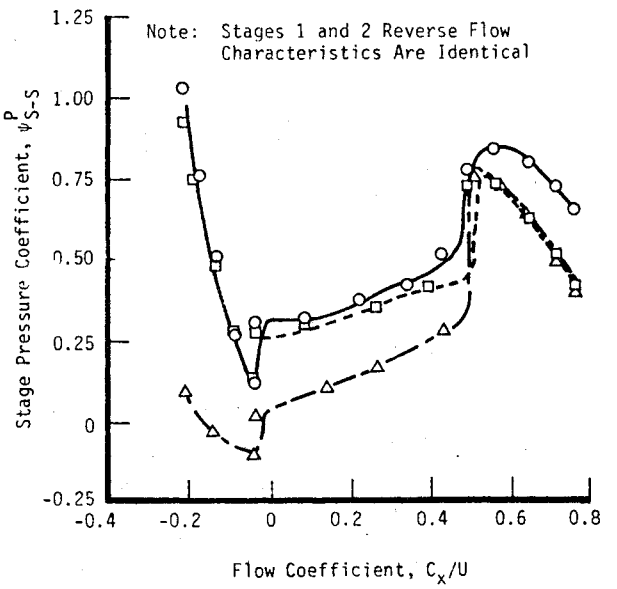

Fig. 3 Synthesized stage characteristics for a three-stage, low speed, experimental compressor rig and comparison to experimental results.

isentropic nozzle model for choked flow is applied at the exit.

A more detailed explanation of the modeling technique can be found in Ref. 14.

Model Operational Verification

For the present studies the modeling technique described in the previous section was employed to develop models of a three-stage, low-pressure, compressor research rig and a single-spool, nine-stage, high-speed compressor typical of the core compressor of a turbofan engine. To completely validate the modeling technique for these applications requires that the models be exercised and compared to experimental results over the range of intended use. However, only limited experimental data, that is, both overall and interstage data while in rotating stall or surge existed for the three-stage compressor. No experimental data for validation were available for the modeled nine-stage compressor. In fact, it was concluded that currently, in the open literature, there is no one set of data for use as a validation vehicle.

The available experimental results from tests of the three-stage, low-speed, compressor research rig of Gamache were utilized.[5] Transient interstage or overall performance data for surge and rotating stall events were not reported. However, steady-state data were available from which stage characteristics could be synthesized. Overall system performance during surge and rotating stall was available from tests of a similar system, reported in Ref. 1. Configuring the model to the compression system is reported in Ref. 5, but comparing it to measured overall dynamic performance from Ref. 1 provided the best available means for qualitative comparisons for "operational verification."

Experimental data for the modeled nine-stage, high-speed compression system were not available, and a model-experiment comparison could not be made. It is noted that the results of a previous qualitative verification of the nine-stage compressor[14] were similar to those presented in this section for the low-speed system.

Three-Stage Rig Simulations

The three-stage, low-speed compressor rig consisted of three nonrepeating stages with a constant cross-sectional area annulus. The hub and tip diameters were 53.63 and 60.96 cm, respectively, which produced a hub-to-tip ratio of 0.88. Gamache's major emphasis was the study of the performance of this compressor rig during steady reversed flow. The rig was configured to hold a constant speed while forcing reversed flow through the compressor. By accomplishing this for many flow points, it was possible to obtain overall and stage performance in the reversed flow region. With the previous work of Eastland,[15] a complete set of steady-state stage pressure characteristics and corresponding overall steady system performance was available for this rig.

A complete temperature rise characteristic was not given for each stage, but energy input to the overall system was given in terms of a torque coefficient. For the present purposes, stage temperature rise characteristics were synthesized as total temperature ratios based upon the overall torque characteristic and two isolated flow points in rotating stall. Temperature characteristics were synthesized which would give the same overall torque as observed experimentally. Lacking any other criteria for stage work division, all stage temperature characteristics were synthesized identically.

Measured stage pressure and synthesized temperature rise characteristics for the three-stage, low-speed, research compressor are presented in Fig. 3. Pressure rise characteristics are based upon reported experimental stage performance measurements which described individual stage pressure behavior during unstalled operation, rotating stall, and reversed flow. Stage temperature rise characteristics have been synthesized as described above.

While the referenced three-stage compression system tests provided excellent stage characteristic data, detailed system behavior during surge and rotating stall was not available from either Refs. 5 or 15. However, this rig was similar to one used in a previous experimental investigation of surge and rotating stall.[1] Both compression systems consisted of three stages with a constant area annulus. The major differences were in the blading. The rig of Ref. 1 incorporated three repeating stages, using NACA 400 series airfoils with a hub-to-tip ratio of 0.7, whereas the rig of Ref. 5 (data used to develop stage characteristics) consisted of three nonrepeating stages with a hub-to-tip ratio of 0.88. The speed capability of both machines was the same. An extensive experimental investigation to determine system response during poststall events for a variety of compressor/plenum configurations was performed with this rig.

The compression system model was configured to the geometry specified for the compressor/plenum rig of Ref. 1, but using the stage characteristics developed by Eastland and Gamache as presented in Fig. 3. For comparison purposes, the "B" parameter was used as a reference variable for both the experimental compressor and the model. The parameter is defined as

$$B = (U/2a)\,(V_p/A_cL_c)^{1/2} \tag{5}$$

The value of the B parameter has been shown to be an indication of whether rotating stall or surge may be expected to occur in a particular compressor.[1]

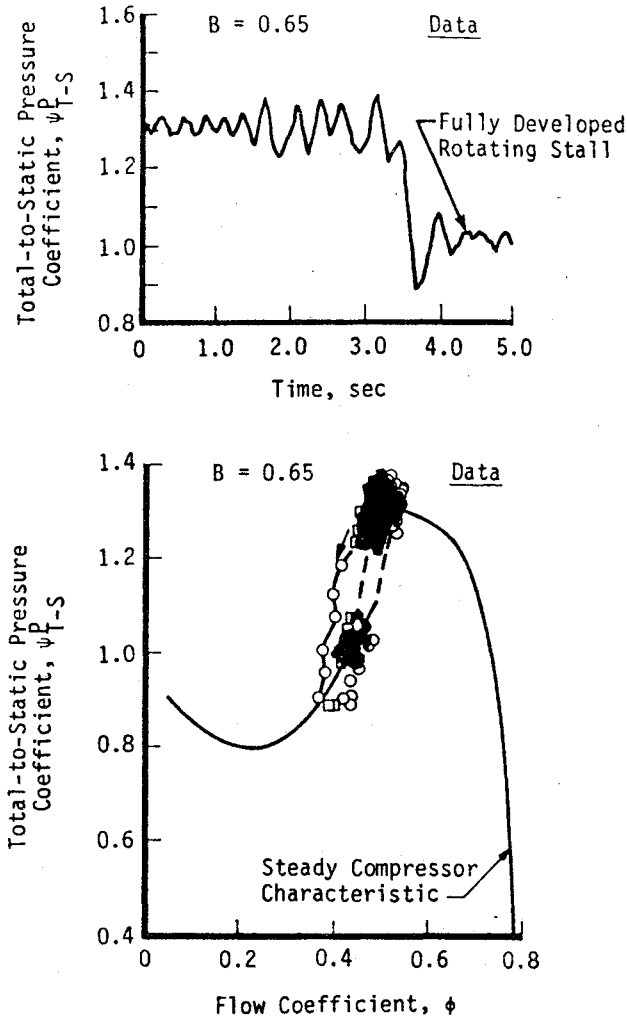

Fig. 4 Poststall behavior of compressor rig: Rotating stall, B = 0.65.

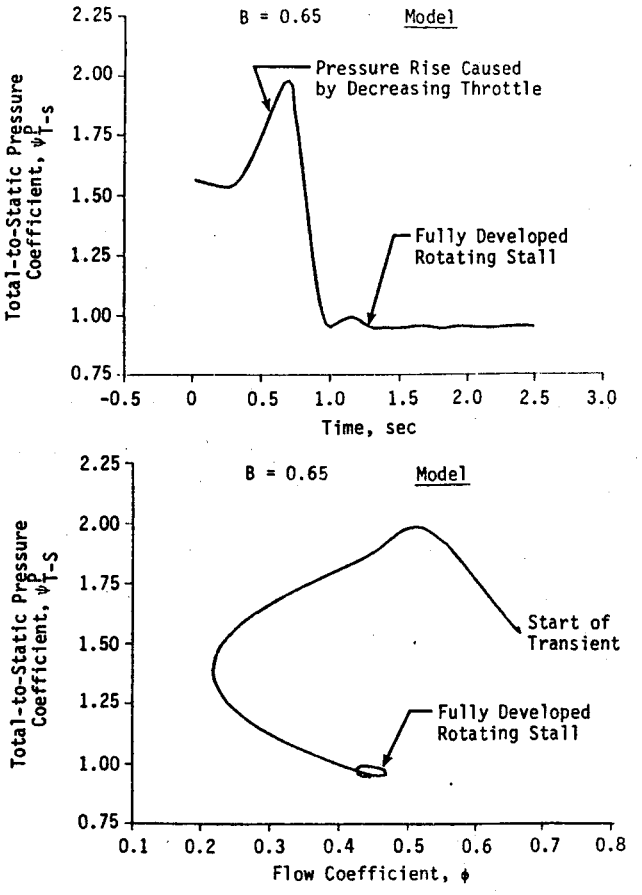

Fig. 5 Three-stage model overall compression system poststall behavior: Rotating stall, $B = 0.65$.

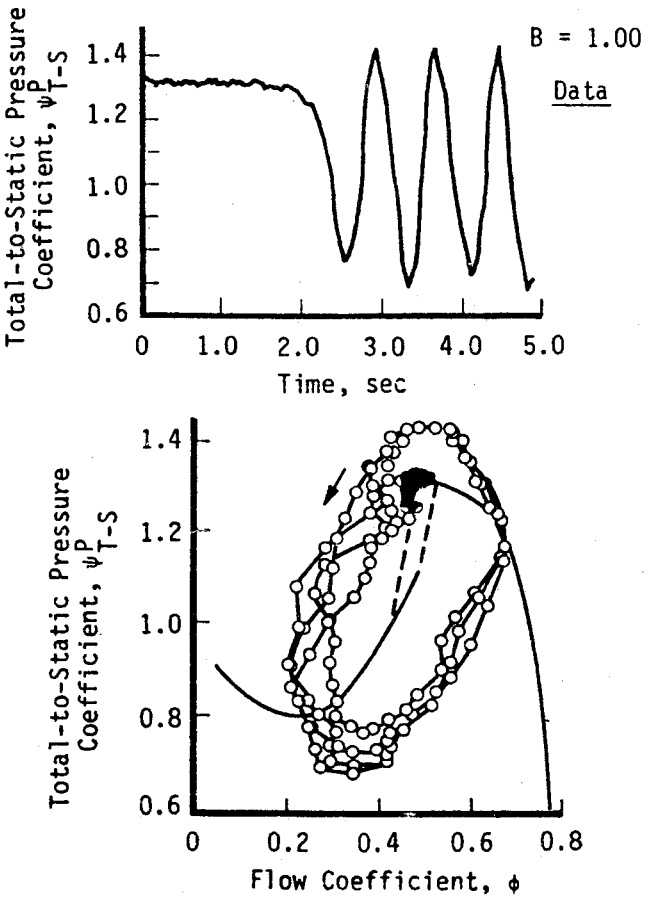

Fig. 6 Poststall behavior of compressor rig: Classic surge, $B = 1.0$.

Three model cases will be compared in this paper to experimental results from Ref. 1, corresponding to B parameters of 0.65, 1.00, and 1.58. These B parameters produced rotating stall, classical surge, and deep surge, respectively, for the system reported in Ref. 1.

Rotating Stall

The first experimental transient was conducted at a B value of 0.65. The compressor rig throttle was slowly closed to the point of instability and then held constant. The system became unstable at the uniform flow stall point and then traversed to rotating stall (Fig. 4).

The compressor model was configured in a similar way to a B parameter value of 0.65 at instability initiation. The model "throttle" was closed just enough to cause instability and then held constant. The compressor blade force dynamic lagging constant, τ, was set at the model boundary between surge and rotating stall such that the overall system performance traversed immediately to the new operating point indicative of fully developed rotating stall. This modeled poststall behavior is presented in Fig. 5. Comparison to the general nature of the experimental results (Fig. 4) indicates correctly simulated overall system behavior.

Classical Surge

In a second test, the compressor rig of Ref. 1 was reconfigured to operate at a B value of 1.00. In this condition, the system exhibited classical surge cycles on the order of 1.5 Hz as presented in Fig. 6.

The dynamic model was reconfigured to produce a B value of 1.00. The blade force time constant, τ, was held to the value determined in the previous simulation. Under these conditions, the model also exhibited surge as presented in Fig. 7. Comparing the time history of the pressure coefficients, one can observe that the change in this parameter is similar in nature and frequency to that observed experimentally (Fig. 6). Comparing the model results as depicted on a compressor map, one can observe that the surge trajectories are circular

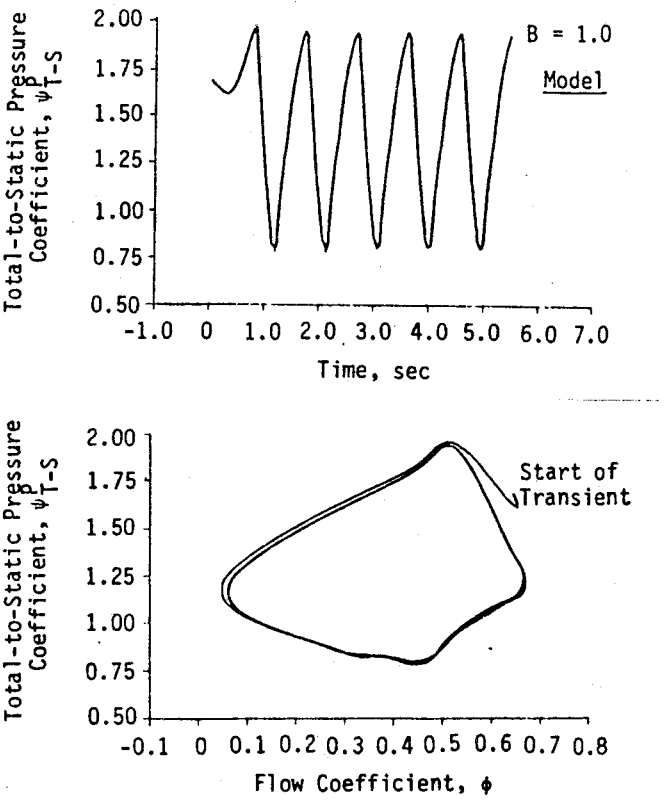

Fig. 7 Three-stage model overall compression system poststall behavior: Classic surge, $B = 1.0$.

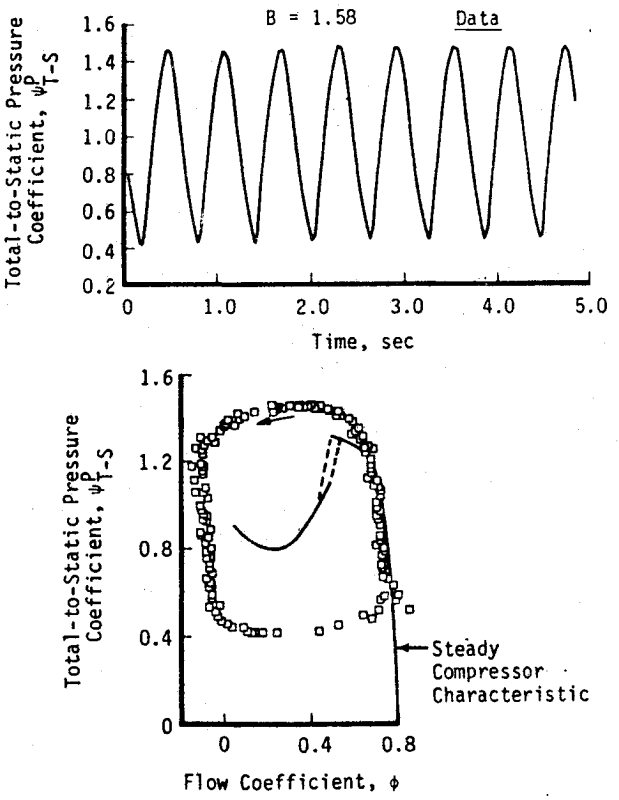

Fig. 8 Poststall behavior of compressor rig: Deep surge, $B = 1.58$.

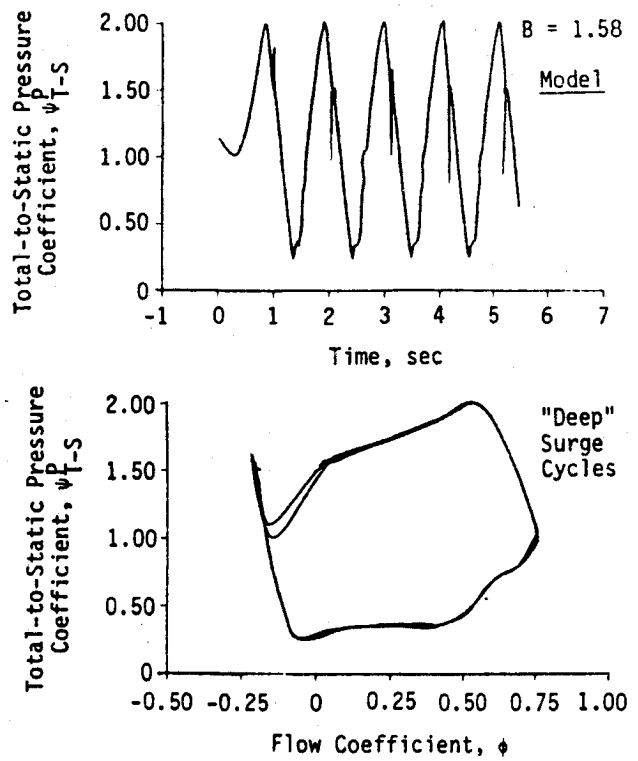

Fig. 9 Three-stage model overall compression system poststall behavior: Deep surge, $B = 1.58$.

in nature and are quite similar to those observed experimentally (Fig. 6).

Deep Surge

The experimental rig of Ref. 1 was operated with a maximum reported B value of 1.58. For this experimental case, a slightly different system behavior was observed. The surge trajectory became larger with near-zero flow during the surge

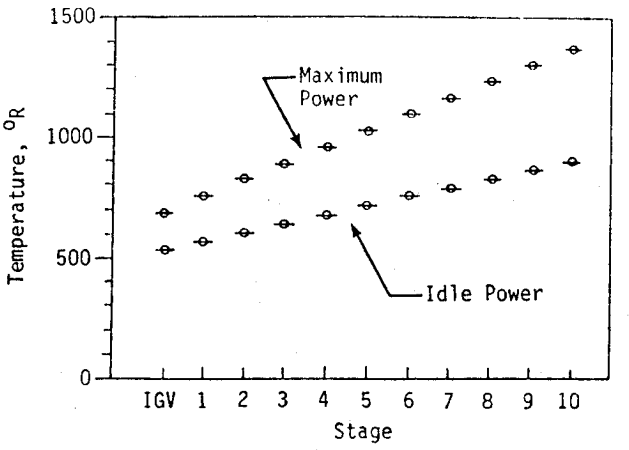

a) Core compressor temperature distribution

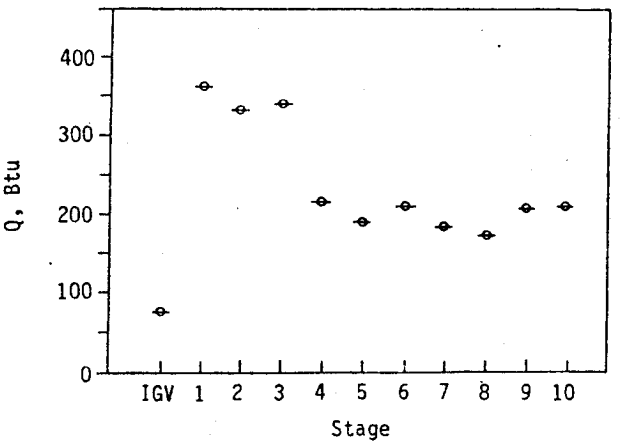

b) Stored thermal energy by stage blading

Fig. 10 Predicted stage temperature distribution at maximum and idle power and corresponding blade stored thermal energy in each stage.

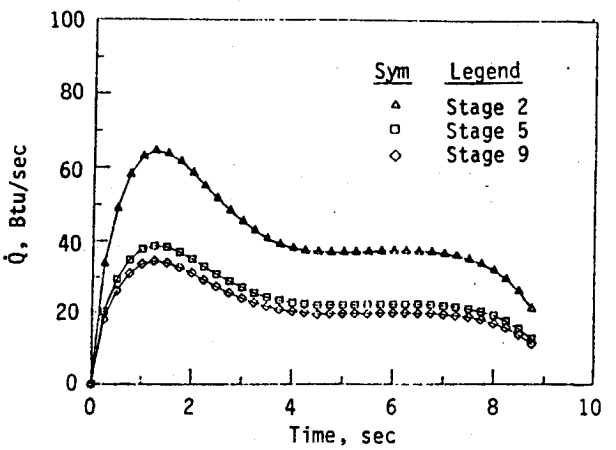

Fig. 11 Typical stage heat transfer rates based upon experimental results.

cycle, but still of the classical type. By decreasing the throttle closure point beyond the initial surge position, it was discovered that the nature of the surge cycles could be affected. Indicated in Fig. 8 are surge cycles for the same compressor configuration ($B = 1.58$), but at a more restrictive throttle setting. This type of surge cycle has been called a deep surge.

The dynamic model was configured for a B value of 1.58. Again, the blade force time constant, τ, was held at the previous value. The simulated throttle was decreased to a value just small enough to cause compression system instability. Resulting overall system response was indicative of the classical type surge as was expected.

Further decreasing the throttle closure to 60% of the minimum value for system instability caused the model to exhibit deep surge, as was observed experimentally. Modeled overall system response is presented in Fig. 9. Model trajectories are indicative of deep surge poststall behavior with a frequency of 1 Hz.

In summary, the modeling technique described herein was operationally verified by comparison with available experimental results. Comparison of model overall performance during postsurge events to the general nature of the experimental results indicated correct simulated overall system behavior.

Parametric Studies

To indicate the unique capabilities and potential usefulness of this stage-by-stage, poststall compression system modeling technique, a parametric study was conducted to assess two different effects: 1) the effect of heat transfer due to rapid power lever transients on system poststall behavior employing the nine-stage model and 2) the effect of tip casing treatment on system behavior using the three-stage model.

Effect of Heat Transfer on Poststall Behavior (Nine-Stage Model)

Operation of high-speed, high-pressure ratio compressors results in a large temperature rise through the compressor. A portion of the large amount of energy input is stored in the compressor blades, rotors, and disks. Thus, during engine throttle transients as in a bodie maneuver (maximum power to idle then back to maximum power), heat transfer between the compressor metal and the airflow takes place. The release of energy during the transient from maximum power to idle causes a change in density, which produces a shift in the compressor characteristic and lowers the stability limit.[16] This loss in surge margin can result in a compression system instability during throttle readvance to maximum power.

From a modeling study, MacCallum and Pilidis[16] concluded that the following thermal effects contribute to the loss in stall margin during reacceleration: nonadiabatic flows causing density changes due to heat transfer; changes in boundary-layer development on the blade airfoils; changes in the boundary-layer development near the end walls; changes in tip clearances; and changes in seal clearances. For this study, only the effect of nonadiabatic flows was considered for analysis.

An investigation by Crawford and Burwell[17] quantified the magnitude and nature of the heat transfer during turbine engine bodie maneuvers using actual engine test results. A calculation of stage thermal energy was made based upon the following equation:

$$Q_{\text{stage}} = mC(T_{\max} - T_{\text{idle}}) \tag{6}$$

where

m = mass of the blades, platforms and seals

C = specific heat of the metal

$T_{\max}$ = stage total temperature at maximum power

T_{idle} = stage total temperature at idle power

Stage temperature distributions were obtained from a stage stacking model simulating idle and max power operation at the flight conditions tested. Stage temperature distributions for maximum and idle power, along with the corresponding stored thermal energy are presented in Fig. 10. With a calculation of transient airflow, heat transfer rates (Btu/Sec) were calculated. Typical stage heat-transfer rates calculated from experimental results obtained from current-day high-pressure compressors are presented in Fig. 11. Using these rates as a guideline, stage heat transfer rates were postulated for a nine-stage compression system which had just completed a bodie transient.

The model was operated to simulate operation at 70% speed with the throttle set such that a compressor instability would occur. The stage force lagging constant, τ, was set at slightly lower value than the model-determined surge/stall boundary to ensure that surge would be the initial poststall event. (Smaller values of τ encourage a surge-like result from the model.) A stage specific heat transfer was chosen for each stage based upon the calculated temperature distribution represented in Fig. 10. Heat-transfer rates were calculated from Eq. 6, and were brought to their maximum level exponentially over a time period of approximately one second, as was indicated experimentally (Fig. 11). The postulated heat-transfer distribution for the nine-stage compressor is illustrated in Fig. 12. Since the throttle was set such that an instability would occur, the heat-transfer rates are shown to be oscillating during the first second of the dynamic event because the compressor was experiencing surge during this period. However, once the stage heat-transfer rates had reached their maximum values, the compressor moved to the nonrecoverable state as illustrated in Fig. 13. Once the nonrecoverable state was reached, heat transfer rates reduced because of the reduction in overall airflow.

This study assumes that a compressor instability will occur during a bodie maneuver and the model was configured to favor this result. Even if such were not the case, the results from the model have indicated that because of the heat transfer generated within the compressor at time of throttle readvance, the compression system may be more likely to enter the nonrecoverable state (rotating stall) when the system is near the surge/rotating stall boundary.

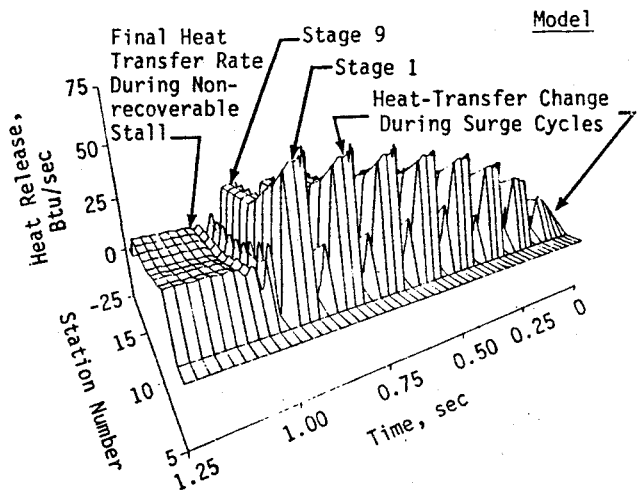

Fig. 12 Heat transfer changes during throttle induced surge cycles of a nine-stage high pressure compressor at 70% speed.

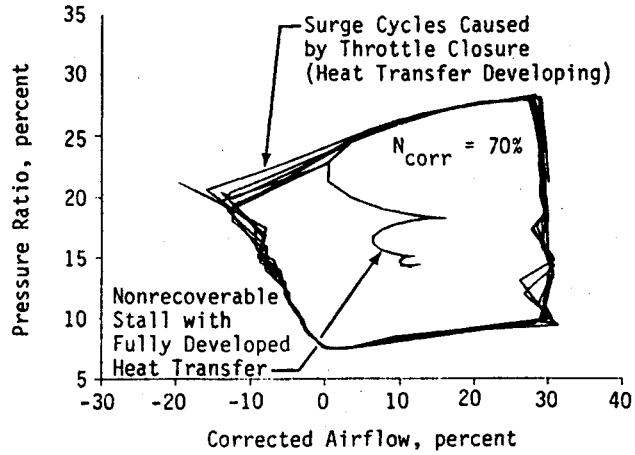

Fig. 13 Effect of compressor heat transfer (blade to gas path) on poststall behavior, nine-stage HPC at 70% speed.

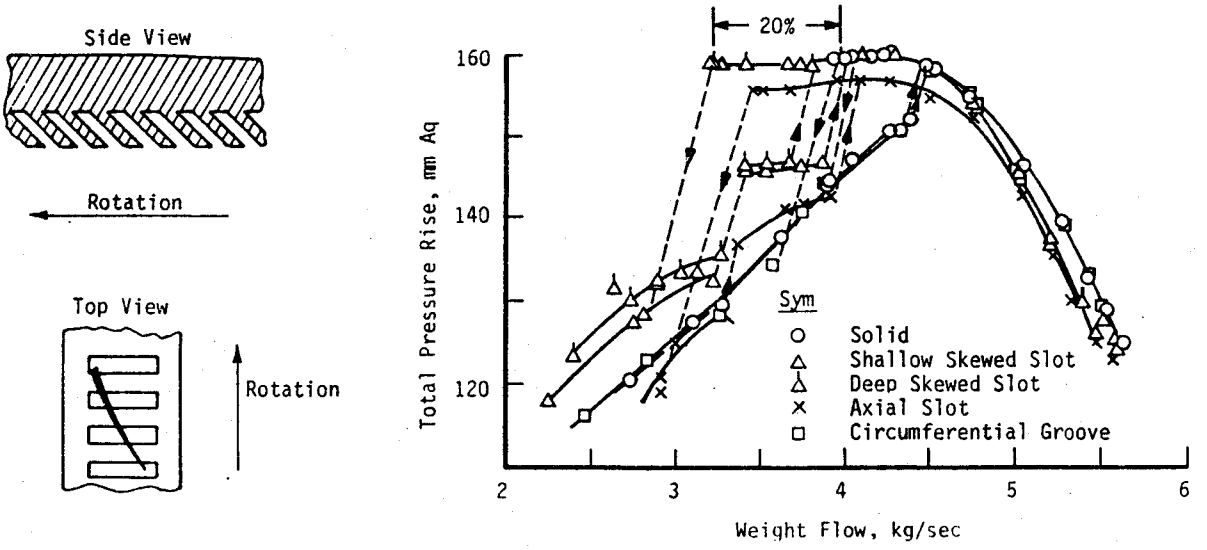

a) Tip treatment modification—Deep skewed slot insert

b) Effects on stage characteristics

Fig. 14 Possible tip treatment modification and its effect on stage characteristics.

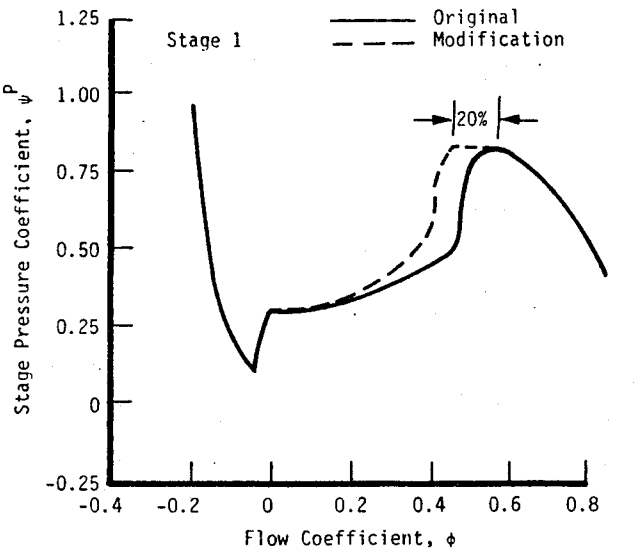

Fig. 15 Postulated stage pressure characteristic modification as a result of tip treatment.

Effect of Tip Casing Treatment on Post-Stall Behavior (Three-Stage Model)

Once a particular compression system is designed and built, the performance and stability behavior are fixed within certain limits. There are only a limited number of external changes that can be made to improve either performance or stability. If these changes cannot produce the desired result, certain internal or blade changes such as camber, stagger, tip clearance or tip casing treatment can be made which improve performance and stability.

A possible change that will be considered is the effect of some type of tip-casing treatment. Takata and Tsukuda,[18] utilizing a low-speed compressor rig, investigated the effects of certain types of tip-casing treatment on the performance of a single rotor row. Of the several types of treatment investigated, they found that a deep-skewed slot tip treatment most improved the stage characteristics. Presented in Fig. 14 is the deep-skewed slot modification and the observed effect on stage performance. Although stage pressure rise is not increased by this technique, the amount of airflow reduction necessary for stall to occur was extended by 20%. This provided more stall margin and reduced the chances for stall occurrence. In addition, a portion of the rotating stall characteristic was presented, which indicated a higher average pressure level during rotating stall.

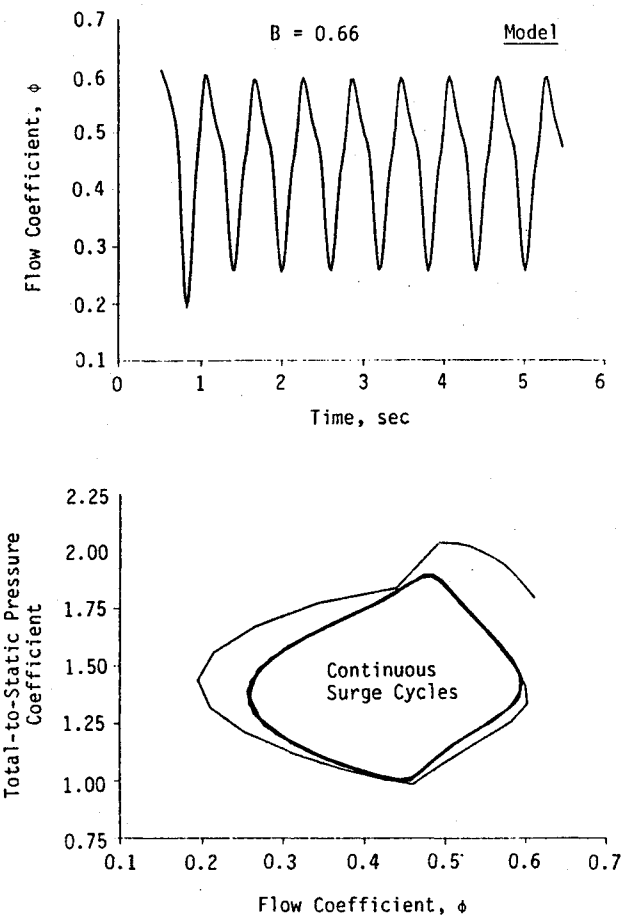

Fig. 16 Model prediction of the effect of first stage tip treatment on poststall behavior: B = 0.65.

To evaluate the effect of such a modification on compression system poststall behavior, the three-stage, low-speed model was chosen for study. A low-speed condition (Fig. 5) was chosen in which rotating stall was the end result. During these hardware modification studies, all variables (B parameter, force lagging constant, τ, speed and plenum configuration)

were held constant except for the changes in the quasi-steady characteristics described below.

Presented in Fig. 15 is a postulated first-stage pressure characteristic with stall margin improvement based upon the results of the deep-skewed tip-casing treatment. The maximum stall point pressure rise is extended for a 20% reduction in airflow, effectively increasing the stall margin for the first stage. The rotating stall characteristic is assumed to be similar to the original shape, but at a higher pressure, as was indicated experimentally. With this change to the first stage only, the modeled compression system exhibited continuous surge cycles, rather than rotating stall, as illustrated in Fig. 16. When similar changes were made to the second and third stages individually, the results were nearly identical. However, when changes to all three stages were incorporated collectively, the compression system resisted the stall condition altogether at the throttle setting which had previously caused instability.

Summary and Conclusions

The objective of the present investigation was to develop and evaluate a compression system model capable of exhibiting detailed system behavior during poststall events. The objective was met by the creation, operational verification, and application of a new one-dimensional, stage-by-stage, compression system model with poststall capability. The model provides a tool for analyzing compression system poststall behavior during surge and rotating stall on a stage-by-stage basis, as well as on the overall system level.

The model solves the nonlinear form of the conservation equations and explicitly treats compressibility. The solution of the momentum and energy equations requires knowledge of stage forces and shaft work not only in prestall operation, but also during the poststall events of surge and rotating stall. Stage forces and shaft work are represented by sets of steady-state stage characteristics (pressure and temperature rise as a function of mass flow rate) that are lagged by a first-order lag equation to provide dynamic characteristics during surge and rotating stall.

The model was operationally verified using a three-stage, low-speed compression system for which experimental (prestall and poststall) stage characteristics were available. Overall system poststall behavior was compared to a very similar system for which poststall system performance results were available. The model correctly represented poststall events which encompassed rotating stall, classical surge, and deep surge.

To illustrate the potential usefulness of this stage-by-stage, poststall compression system model, two parametric studies were conducted: one to assess the influence of heat transfer present during rapid power lever transients and a second to assess the effects of a possible hardware modification on compression system poststall behavior. Results from these parametric studies provided additional insight on the effects of compression system behavior during poststall events.

Acknowledgments

The work described herein was sponsored by the Arnold Engineering Development Center (AEDC), Air Force Systems Command. The results were obtained by Sverdrup Technology, Inc., AEDC Group, operating contractor for the propulsion test facilities of the AEDC, Arnold Air Force Base, Tennessee.

References

[1]Greitzer, E. M., "Surge and Rotating Stall in Axial Flow Compressors-Part II: Experimental Results and Comparison with Theory," *ASME Journal of Engineering for Power*, Vol. 98, April 1976, pp. 199–217.

[2]Day, I. J., "Axial Compressor Stall," Ph.D. Dissertation. Christ's College, Cambridge Univ., Cambridge, England, UK, 1976.

[3]Burwell, A. E., and Patterson, G. T., "Dynamic Engine Behavior During Post Surge Operation of a Turbofan Engine," AIAA/SAE/ASME/ASEE 21st Joint Propulsion Conference, AIAA Paper 85-1430, Monterey, CA, July 8–10, 1985.

[4]French, J. V., "Modeling Post-Stall Operation of Aircraft Gas Turbine Engines," AIAA/SAE/ASME/ASEE 21st Joint Propulsion Conference, AIAA Paper 85-1431, Monterey, CA, July 8–10, 1985.

[5]Gamache, R. N., "Axial Compressor Reversed Flow Performance," Ph.D. Dissertation, Massachusetts Inst. of Technology, May 1985.

[6]Kimzey, W. F., "An Analysis of the Influence of Some External Disturbances on the Aerodynamic Stability of Turbine Engine Axial Flow Fans and Compressors," Arnold Engineering Development Center TR-77-80 (AD-AO43543), Arnold AFS, TN, Aug. 1977.

[7]Davis, M. W., Jr., "A Stage-by-Stage Dual-Spool Compression System Modeling Technique," ASME Gas Turbine Conference, ASME Paper 82-GT-189, London, England, March 1982.

[8]Tesch, W. A., and Steenken, W. G., "Blade Row Dynamic Digital Compressor Program, Vol. 1, J85, Clean Inlet Flow and Parallel Compressor Models," NASA CR-134978, Lewis Research Center, Cleveland, OH, March 1976.

[9]Sugiyama, Y., Hamed, A., and Tabakoff, W., "A Study on the Mechanism of Compressor Surge Due to Inlet Pressure Disturbances," 16th Aerospace Sciences Meeting, AIAA Paper 78-246, Huntsville, AL, Jan. 1978.

[10]Greitzer, E. M., "Surge and Rotating Stall in Axial Flow Compressors-Part I: Theoretical Compression System Model," *ASME Journal of Engineering for Power*, Vol. 98, April 1976, pp. 190–198.

[11]Moore, F. K., and Greitzer, E. M., "A Theory of Post-Stall Transients in Axial Compression Systems: Part I-Development of Equations," 30th International Gas Turbine Conference, ASME Paper 55-GT-171, Houston, TX, March 1985.

[12]Takata, H., and Nagano, S., "Nonlinear Analysis of Rotating Stall," *Journal of Engineering for Power*, Oct. 1972.

[13]MacCormack, R. W., "The Effect of Viscosity in Hypervelocity Impact Cratering," AIAA Hypervelocity Impact Conference, AIAA Paper 69-354, Cincinnati, OH, April 30–May 2, 1969.

[14]Davis, M. W., Jr., "A Stage-by-Stage Post-Stall Compression System Modeling Technique: Methodology, Validation and Application," Ph.D. Dissertation, Virginia Polytechnic Inst. and State Univ., Dec. 1986.

[15]Eastland, A. H. J., "Investigation of Compressor Performance in Rotating Stall: I—Facility Design and Construction and Initial Steady State Measurements," MIT Gas Turbine and Plasma Dynamics Lab. Rept. 164, June 1982.

[16]MacCallum, H. R. L., and Pilidis, P., "The Prediction of Surge Margins During Gas Turbine Transients," ASME Gas Turbine Conference, ASME Paper 85-GT-208, Houston, TX, March 1985.

[17]Crawford, R. A., and Burwell, A. E., "Quantitative Evaluation of Transient Heat Transfer on Axial Flow Compressor Stability," AIAA/SAE/ASME/ASEE 21st Joint Propulsion Conference, AIAA Paper 85-1352, Monterey, CA, July 1985.

[18]Takata, H., and Tsukuda, U., "Stall Margin Improvement by Casing Treatment—Its Mechanism and Effectiveness," *Journal of Engineering for Power*, Jan. 1977.